Immune complex solubility and size govern Fc-gamma receptor responses

Haizhang Chen[1,2], Andrea Maul-Pavicic[3,4], Martin Holzer[5], Ulrich Salzer[3], Nina Chevalier[3], Reinhard E. Voll[3,4], Hartmut Hengel[1,2,*] & Philipp Kolb[1,2,*]

[1]Institute of Virology, University Medical Center, Albert-Ludwigs-University Freiburg, Hermann-Herder-Str. 11, 79104 Freiburg, Germany

[2]Faculty of Medicine, Albert-Ludwigs-University Freiburg, 79104 Freiburg, Germany

[3]Department of Rheumatology and Clinical Immunology, Medical Center - University of Freiburg, Faculty of Medicine, University of Freiburg, Hugstetterstr. 55, 79106 Freiburg, Germany

[4]Center for Chronic Immunodeficiency (CCI), Medical Center-University of Freiburg, Faculty of Medicine, University of Freiburg, Breisacherstr. 115, 79106 Freiburg, Germany

[5]Institute for Pharmaceutical Sciences, Albert-Ludwigs-University Freiburg, Hermann-Herder-Str. 9, 79104 Freiburg, Germany

*corresponding authors (Hartmut.hengel@uniklinik-freiburg.de)

One Sentence Summary: This study reveals selective activation of individual Fc-gamma receptors by soluble but not immobilized immune complexes, establishing a novel biomarker for autoimmune disease in humans and mouse models.

Abstract: Fc-gamma receptor (FcγR) activation by soluble IgG immune complexes (sICs) is thought to be a major mechanism of inflammation in certain autoimmune diseases such as systemic lupus erythematosus (SLE). A robust and scalable test system allowing for the detection and quantification of sIC bioactivity is missing. Therefore, we developed a comprehensive reporter cell panel capable of measuring the sIC-mediated activation of individual human and mouse FcγRs. We show that compared to human FcγRs IIB and III, human FcγRs I and IIA lack sensitivity to sICs. Further, the assay proved to be sensitive to sIC stoichiometry and size enabling us to demonstrate for the first time a complete translation of the Heidelberger-Kendall precipitation curve to FcγR responsiveness. This was validated using primary immune cells. The approach was applied to quantify sIC-mediated FcγR activation using sera from SLE patients or from mouse models of lupus and arthritis. Thus, in clinical practice, it can be employed as a toolbox enabling the evaluation of FcγR activation by sICs as a biomarker for disease activity in immune-complex mediated diseases.

Introduction

Immunoglobulin G (IgG) is the dominant immunoglobulin isotype in chronic infections and in antibody-mediated autoimmune diseases. The multi-faced effects of the IgG molecule rely both on the F(ab) regions, which recognize a specific antigen to form immune complexes (ICs), and the constant Fc region (Fcγ), which is detected by Fcγ receptors (FcγRs) found on most cells of the immune system (*1*). When IgG binds to its antigen ICs are formed, which, depending on the respective antigen, are either cell-bound or soluble (sICs). The composition of sICs is dependent on the number of epitopes recognized by IgG on a single antigen molecule and the ability of the antigen to form multimers. Fcγ-FcγR binding is necessary but not sufficient to activate FcγRs since physical receptor cross-linking generally underlies receptor activation (*2-5*). Firmly fixed cell bound ICs are readily able to cross-link FcγRs (*4, 6*). This condition induces various signaling pathways (*7-9*) which in turn regulate immune

cell effector functions (*10, 11*). It is also suggested that sICs can dynamically tune FcγR triggering, implying that changes in sIC size directly impact FcγR responses (*6*). However, the molecular requirements are largely unknown. Also, a functional reproduction of the paradigmatic Heidelberger-Kendall precipitation curve, describing that the molecular size of sICs determined by the antibody:antigen ratio dynamically tunes FcγR activation on and off (*12, 13*), is so far missing.

In contrast to FcγR binding of monomeric ligands without consequences, IC-mediated FcγR cross-linking initiates the full signal cascade followed by immune cell activation or inhibition, resp. (*5, 8, 14, 15*). Human FcγRs are membrane resident receptors recognizing Fcγ. Among all type I FcγRs, FcγRIIB (CD32B) is the only inhibitory one signaling via immunoreceptor tyrosine-based inhibitory motifs (ITIMs) while the activating receptors are associated with immunoreceptor tyrosine-based activation motifs (ITAMs). Another exception is FcγRIIIB (CD16B), which is glycosylphosphatidylinositol (GPI)-anchored (*16-19*). FcγRI (CD64) is the only receptor with high affinity binding to monomeric IgG not associated with antigen and is primarily tasked with phagocytosis linked to antigen processing and pathogen clearance (*20, 21*). All the other FcγRs only efficiently bind to complexed, meaning antigen-bound IgG (*1, 16, 17*). While FcγRI, FcγRIIB and FcγRIIIA are able to recognize sICs, this has not been reported for FcγRIIA (CD32A), rather this receptor has recently been shown to depend on the neonatal Fc receptor (FcRn) or FcγRIIIB (CD16B) to do so (*22, 23*). Activation of FcγRs leads to a variety of cellular effector functions such as antibody-dependent cellular cytotoxicity (ADCC) by natural killer (NK) cells via FcγRIIIA, antibody-dependent cellular phagocytosis (ADCP) by macrophages via FcγRI, cytokine and chemokine secretion by NK cells and macrophages via FcγRIIIA. Further effector responses are reactive oxygen species (ROS) production of neutrophils and neutrophil extracellular traps formation (NETosis) via FcγRIIIB, dendritic cell (DC) maturation and antigen presentation via FcγRIIA and B cell selection and differentiation via FcγRIIB (*10, 24-30*). Consequently, FcγRs connect and

76 regulate both innate and adaptive branches of the immune system. Various factors have been
77 indicated to influence the IC-dependent FcγR activation profiles, including Fcγ-FcγR binding
78 affinity and avidity (*31*), IgG subclass, glycosylation patterns and genetic polymorphism (*4,*
79 *24, 25, 32*), stoichiometry of antigen-antibody-ratio (*6, 30, 33*) and FcγR clustering patterns
80 (*34*). Specifically, Asn297-linked glycosylation patterns of the IgG Fc domain initiate either
81 pro- or anti-inflammatory effector pathways by tuning the binding affinity to activating versus
82 inhibitory FcγRs, respectively (*35*). However, despite being explored in proof-of-concept
83 studies, the functional consequences of these ligand features on a specific receptor are still not
84 fully understood. Therefore, an assay platform allowing for the systematic functional
85 assessment of IC-mediated FcγR activation is strongly required. While a previously
86 developed cell-based assay addresses sIC-mediated activation of the inhibitory FcγRIIB (*36*),
87 a platform allowing for the comprehensive analysis of all FcγRs is missing.
88 sICs and immobilized ICs represent different stimuli for the immune system (*22, 29*). Soluble
89 circulating ICs are commonly associated with certain chronic viral or bacterial infections (*37,*
90 *38*) and autoimmune diseases, such as systemic lupus erythematosus (SLE) or rheumatoid
91 arthritis (RA) (*39-41*). When accumulating and deposited in tissues sICs can cause local
92 damage due to inflammatory responses, classified as type III hypersensitivity (*42*). Typically,
93 sICs related disorders are characterized by systemic cytokine secretion which can be followed
94 by immune cell exhaustion and senescence (*43, 44*). In order to study sIC-dependent
95 activation of FcγRs in detail, we employed a cell-based assay which has been previously
96 utilized to study immobilized ICs (*45*) and adapted it into a sIC sensitive reporter system
97 capable of distinguishing the activation of individual FcγRs and their responses to varying
98 complex size. This approach allowed for the first time a complete reproduction of the
99 Heidelberger-Kendall precipitation curve measuring actual FcγR triggering. The assay
100 enables a quantification of clinically relevant sICs in sera from SLE patients and autoimmune-

101 prone mice with immune-complex-mediated arthritis and lupus using reporter cells expressing
102 chimeric mouse FcγRs.
103
104 **Results**
105 *Experimental assay setup*
106 The assay used in this study was adapted from a previously described cell-based FcγR
107 activation assay designed to measure receptor activation in response to opsonized virus
108 infected cells (*45*) or therapeutic Fc-fusion proteins (*46*). We complemented the assay setup to
109 enable measurement of sICs when incubated with reporter cells stably expressing the
110 ectodomains of the human FcγR fused to the signaling module of the mouse CD3-ζ chain
111 (FcγRI: Acc# X14356; FcγRIIA(R): Acc# X62572; FcγRIIB/C: Acc# X52473; FcγRIIIA(V):
112 Acc# LT737365). Ectodomains of FcγRIIB and FcγRIIC are identical. Second generation
113 reporter cells were generated to improve stable expression of chimeric FcγRs compared to the
114 transfectants used in the original assay (*45*). To this end, BW5147 cells were transduced as
115 described previously via lentiviral transduction (*45, 47*). Human FcγR expression on
116 transduced cells after puromycin selection is shown in Fig. 1A. FcγR triggering is translated
117 into activation of the reporter cells and measured by quantification of endogenous IL-2 (mIL-
118 2) secretion into the cell culture supernatant using an anti-IL-2 sandwich ELISA as described
119 previously (*45*). In order to employ the original assay, designed to detect ICs on adherent
120 virus-infected cells, for the detection of soluble ICs we first determined the suspension of IgG
121 achieved by pre-incubating a 96 well ELISA microtiter plate with PBS/FCS blocking buffer.
122 To this end, we compared graded concentrations of FCS in the blocking reagent and measured
123 the threshold at which IgG (rituximab, Rtx) was no longer adsorbed to the plate and stayed
124 abundantly in solution. Fig. 1B demonstrates that FCS supplementation to 1% (v/v) or higher
125 is sufficient to keep IgG antibodies in solution and prevents binding to the plastic surface.
126 Using this adapted protocol, the assay now allowed for the sensitive detection and

127 characterization of FcγR interaction with immobilized ICs versus sICs as shown
128 schematically in Fig. 1C. First, we set out to test if monomeric IgG upon immobilization
129 becomes an operational surrogate for IgG-opsonized cells or immobilized ICs with regard to
130 FcγR activation as suggested before (*48*). As depicted in Fig. 2, there was no qualitative
131 difference in FcγR activation between immobilized Rtx, immobilized ICs (Rtx + rec. CD20)
132 or Rtx-opsonized 293T-CD20 cells, showing that FcγR cross-linking by clustered IgG alone is
133 sufficient for receptor cross-linking and activation. In contrast, sICs formed by monomeric
134 CD20 peptide (aa 141-188) and Rtx failed to activate FcγRs even at very high ligand
135 concentrations. Based on this finding we hypothesized that, in order to generate sICs able to
136 activate FcγRs, antigens have to be multivalent to achieve cross-linking of FcγRs. Of note, to
137 reliably and accurately differentiate between soluble and immobilized triggers using this
138 assay, reagents for the generation of ICs need to be of very high purity and consistent
139 stability. Indeed, only combinations of pharmaceutical therapy grade, i.e. ultra-pure mAbs and
140 pure antigens (purified via size exclusion chromatography) showed reproducible, dose-
141 dependent and specific activation in the reporter assay (data not shown).
142
143 *Quantification of human FcγR responsiveness to multimeric sICs*
144 To date, there are only few commercially available human IgG-antigen pairs that meet both
145 the above mentioned high grade purity requirements while also providing a multimeric
146 antigen. In order to meet these stipulations of ultra-pure synthetic soluble immune complexes
147 we focused on three pairs of multivalent antigens and their respective mAbs that were
148 available in required amounts enabling large-scale titration experiments; trimeric
149 rhTNFα:IgG1 infliximab (TNFα:Ifx), dimeric rhVEGFA: IgG1 bevacizumab (VEGFA/Bvz)
150 and dimeric rhIL-5: IgG1 mepolizumab (IL-5/Mpz). As lymphocytes express TNFα-receptors
151 I and II while not expressing receptors for IL-5 or VEGFA, we tested whether the mouse
152 lymphocyte derived BW5147 thymoma reporter cell line is sensitive to high concentrations of

153 rhTNFα. Toxicity testing revealed that even high concentrations up to 76.75 nM rhTNFα did
154 not affect viability of reporter cells (Fig. S1). Next, we measured the dose-dependent
155 activation of human FcγRs comparing immobilized IgG to soluble ICs using the FcγR
156 reporter cell panel (Fig. 3). Soluble antigen or mAb alone served as negative controls showing
157 no background activation even at high concentrations. Immobilized rituximab served as a
158 positive control for inter-experimental reference. We observed that all FcγRs are strongly
159 activated in a dose-dependent manner when incubated with immobilized IgG. Incubating the
160 FcγR reporter cells with sICs at identical molarities showed FcγRIIB/C and FcγRIIIA to be
161 efficiently activated by sICs, while in contrast, FcγRIIA and FcγRI did not respond to sICs.
162 We furthermore observed FcγRIIIA to be efficiently activated by sICs with responses even
163 surpassing those achieved with immobilized IgG for TNFα/Ifx and IL-5/Mpz ICs. FcγRIIB/C
164 showed a generally weaker reactivity towards sICs compared to immobilized ICs, especially
165 at high concentrations whereas an inversion of this order was seen for TNFα/Ifx and
166 VEGFA/Bvz ICs at lower concentrations. IL-5/Mpz, FcγRIIB/C and FcγRIIIA showed
167 similar responsiveness towards immobilized or sICs with a generally stronger activation on
168 immobilized ICs. These findings demonstrate that sICs of different composition vary in the
169 resulting FcγR activation pattern, most likely due to the antigens being either dimeric, trimeric
170 or different in size. As we observed differences in responses to sICs vs. immobilized ICs for
171 individual FcγR-ζ reporter cells, this indicates that FcγR ectodomains alone are already able
172 to differentiate between these triggers. To validate this observation in principle, we
173 determined FcγRIIIA activation using primary human NK cells isolated from PBMCs of
174 healthy donors. NK cells were chosen as they mostly express only one type of FcγR similar to
175 our reporter system. Measuring a panel of activation markers and cytokine responses by flow
176 cytometry, we observed a differential activation pattern depending on ICs being soluble or
177 immobilized at equal molarity (Fig. 4A). We chose IL-5/Mpz sICs as NK cells do not express
178 the IL-5 receptor. While MIP1-β responses were comparable between the two triggers,

179 degranulation (CD107a) and TNFα responses showed a trend towards lower activation by
180 sICs compared to immobilized IgG (Mpz). Strikingly, IFNγ responses were significantly
181 weaker when NK cells were incubated with sICs compared to immobilized IgG. In order to
182 confirm this hierarchy of responses and to enhance the overall low activation by Fcγ
183 compared to the PMA control, we changed the IC setup by generating reverse-orientation
184 sICs consisting of human FcγR-specific mouse mAbs and goat-anti-mouse IgG $F(ab)_2$
185 fragments. NK cell activation by reverse sICs was compared to NK cell activation by
186 immobilized FcγR specific mAbs (Fig. 4B). Here, we not only confirm our previous
187 observations regarding MIP-1β and IFNγ, but we also confirm significantly lower TNFα and
188 CD107a responses towards soluble complexes compared to immobilized mAbs. Importantly,
189 these experiments validate that sICs readily activate primary NK cells and induce
190 immunological effector functions. As in roughly 10% of the population NK cells express
191 FcγRIIC (*49-52*), we also tested if this receptor plays a role in our measurements. Using the
192 same three donors and an FcγRII specific mAb as described above, we did not observe an
193 FcγRII-mediated response. Accordingly, we conclude that FcγRIIC expression did not play a
194 role in our experiments (Fig. 4C). Taken together, we show that multivalent but not dimeric
195 soluble immune complexes govern primary NK cell response and FcγRIIIA activation (Fig.
196 2A).
197
198 *Measurement of FcγR activation in response to changing sIC size*
199 We observed that the dimeric sIC CD20:Rtx molecule complex completely failed to trigger
200 FcγRs, while potentially larger sICs based on multimeric antigens showed an efficient dose-
201 dependent FcγR activation. In order to determine whether BW5147 FcγR-ζ reporter cells are
202 able to respond to changes in sIC size, we tested cross-titrated amounts of antibody (mAb,
203 infliximab, Ifx) and antigen (Ag, rhTNFα). To this end, the reporter cells were incubated with
204 sIC of different mAb:Ag ratios by fixing one parameter and titrating the other. According to

205 the Heidelberger-Kendall precipitation curve (*12*) describing sIC size as being dependent on
206 the mAb:Ag ratio, this should result in varying sIC sizes as an excess of either antigen or
207 antibody results in the formation of smaller complexes compared to the large molecular
208 complexes formed at around equal molarity. Changes in sIC size due to a varying mAb:Ag
209 ratio were quantified using asymmetrical flow-field flow fractionation (AF4) (Fig. 5A and
210 Table S1). Fig. S2 shows a complete run of such an analysis. AF4 analysis identifies the
211 highest sIC mean molecular being approximately 2130 kDa at a 1:3 ratio (mAb Ifx : Ag TNF-
212 α) with sICs getting smaller with increasing excess of either antigen or antibody,
213 recapitulating a Heidelberger-Kendall-like curve. Incubation of the FcγR reporter cells with
214 ICs of varying size indeed shows that the assay is sensitive to exactly monitor changes in sIC
215 size (Fig. 5B). Accordingly, both FcγR types showed the strongest responses at mAb:Ag
216 ratios of approximately 1:3. We then set out to test the accuracy of our reporter cell assay as a
217 surrogate for primary human immune cells expressing FcγRs. To this end, we tested primary
218 NK cells from three individual donors and measured NK cell MIP1-β upregulation in
219 response to synthetic sICs of varying size and composition again using a similar assay setup
220 optimized for NK cell activation. We chose MIP-1β upregulation as a cell surface marker to
221 measure NK cell activation as it showed the highest responsiveness in previous experiments
222 (Fig. 4). We could observe that primary immune cells expressing FcγRIIIA respond to IC
223 size, confirming our assay to be an accurate surrogate for primary immune cell responses to
224 soluble ICs (Fig. 5C). Convincingly, NK cell responses to sICs generated from trimeric
225 antigen (rhTNFα) peaked at a different mAb:Ag ratio compared to NK cell responses to sICs
226 generated from dimeric antigens (rhIL-5 and rhVEGFA). Of note, TNFα and VEGFA activate
227 resting NK cells thus leading to higher MIP1-β positivity when NK cells are incubated in the
228 presence of excess antigen. As NK cells do not express IL-5 receptor, this effect is not
229 observed in the presence of excess IL-5. Regarding TNFα, NK cells still show a stronger
230 activation by sICs generated under optimal mAb:Ag ratios compared to conditions where

231 excess antigen is used. The data reveal a direct correlation between sIC size and effector
232 responses. Conversely, when changing antibody concentrations using fixed amounts of
233 antigen, a consistent reduction of NK cell activation is observed in the presence of excess IgG
234 for all three mAb/Ag pairs.
235
236 *Quantification of sIC bioactivity in sera of SLE patients*
237 In order to apply the assay to a clinically relevant condition associated with the occurrence of
238 sICs we measured circulating sICs present in the serum of SLE patients with variable disease
239 activity. Sera from 4 healthy donors and 25 SLE patients were investigated for FcγRIIIA and
240 FcγRIIB/C activation. Reporter cells readily produced IL-2 in response to patient sera in a
241 dose-dependent manner (shown exemplarily for some SLE patients, see Fig. 6A), which was
242 not the case when sera from healthy controls were tested. Consistent with the observation that
243 FcγRI and FcγRIIA do not respond to synthetic sICs, reporter cells expressing these receptors
244 did also not respond to the tested serum samples (Fig. 6A, lower panel). While this reaction
245 pattern already indicated that sICs are the reactive component measured in SLE patients' sera,
246 we further demonstrate that FcγRIIIA and FcγRIIB/C activation depends on the presence of
247 serum ICs by analyzing patient serum before and after polyethylene glycol (PEG)
248 precipitation and depletion of sICs (Fig. 6B). Next, we calculated the area under the curve
249 (AUC) values for all 25 SLE patient titrations and normalized them to the AUC values
250 measured for healthy individuals. The resulting index values were then correlated with
251 established biomarkers of SLE disease activity, such as anti-dsDNA titers (α-dsDNA) and
252 concentrations of the complement cleavage product C3d (Fig. 6C). We observed a significant
253 correlation between our FcγRIIIA activation index values and both of the determined disease
254 activity markers, anti-dsDNA titers and C3d concentration ($p=0.0465$ and $p=0.0052$,
255 respectively). FcγRIIB/C on the other hand showed no significant correlation with either
256 biomarker. We assume these interrelations may be due to the influence of IgG sialyation

257 found to be reduced in active SLE (*53*). Generally, de-sialylation of IgG leads to stronger
258 binding by the activating receptors FcγRI, FcγRIIA and FcγRIII while it reduces the binding
259 affinity of the inhibitory FcγRIIB (*54*). In sum, our assay allows the indirect quantification of
260 clinically relevant sICs in sera of SLE patients.
261
262 *Assay application to clinically relevant in vivo lupus and arthritis mouse models*
263 BW5147 reporter cells stably expressing chimeric mouse as well as rhesus macaque FcγRs
264 have already been generated using the here described methodology and were successfully
265 used to measure FcγR activation by opsonized adherent cells in previous studies (*47, 55*)
266 (mFcγR reporter cells). As the human FcγR reporter cells described here are sensitive to
267 certain sICs, we next aimed to translate the assay to clinically relevant animal models. To this
268 end, we incubated previously described FcγR reporter cells expressing chimeric mouse FcγRs
269 (*47*) with sera from lupus (NZB/WF1) or arthritis (K/BxN) mice with active autoimmune
270 disease. The reporter assay was performed as described above. We chose to measure the
271 stimulation of the activating receptors, mFcγRIII and mFcγRIV, that correspond to human
272 FcγRIII and show a similar cellular distribution and immune function (*16*). Incubation with
273 synthetic sICs generated from rhTNFα and mouse-anti-hTNFα IgG1 showed both of the
274 mFcγR reporter cells to be equally responsive to sICs (Fig. 7A). Parental BW5147 cells
275 expressing no FcγRs served as a control. The sera of three mice per group were analysed and
276 compared to sera from wildtype C57BL/6 mice, which served as a healthy control. C57BL/6
277 mice were chosen, as healthy K/BxN or NZB/WF1 mice cannot be reliably defined. This is
278 due to the unpredictable disease progression in these mouse models starting from a young age.
279 We consistently detected mFcγR activation by sera from K/BxN or NZB/WF1 compared to
280 C57BL6 mice (Fig. 7B). While the mFcγRIII responses were generally high and similar
281 between K/BxN and NZB/WF1 mice, mFcγRIV responsiveness attended to be lower and
282 individually more variable. Altogether, the assay enables the reliable detection of sICs in sera

283 of mice with immune-complex mediated diseases making it a promising novel tool to monitor
284 sICs as a biomarker of disease activity.
285
286 **Discussion**
287 In this study we established, validated and applied a new assay system that is able for the first
288 time to selectively detect soluble multimeric immune complexes as discrete ligands of FcγR.
289 Major findings are i) that sICs cross-link and trigger human FcγRs IIB/C and IIIA but are
290 neglected by activating FcγRI and IIA; ii) that sICs potency is strictly stoichiometry- and size-
291 dependent and thus reproducing the classical Heidelberger-Kendall curve iii) that the overall
292 functional design of FcγRs is adapted to physical cross-linking by soluble vs. membrane-
293 bound immune complexes. The new test system has various obvious applications in medicine
294 and pharmacy.
295
296 *A novel assay for the quantification of disease-associated as well as synthetic sICs*
297 The new approach presents an important and implementable advancement in immunological
298 methodology as it enables the sensitive detection of receptor-activating ICs by a relatively
299 simple, scalable *in vitro* bioassay with high-throughput potential. Based on our pilot study
300 demonstrating that the sIC-mediated FcγRIIIA activation correlated with SLE disease
301 markers, this is of great value for larger prospective clinical studies in patients with
302 autoimmune diseases such as systemic lupus erythematosus (SLE) and rheumatoid arthritis
303 (RA), where circulating ICs have long been shown to crucially contribute to tissue damage
304 and disease manifestations (*40, 41, 56-58*). Disease-associated, endogenous sICs can also
305 occur during infection, e.g. generated after antibody-mediated destruction of pathogenic
306 viruses or microbes or probably more likely due to the oligomeric nature of numerous viral
307 and bacterial structural proteins generated e.g. by SARS-CoV2 (*59-61*) HIV and hepatitis B
308 virus (HBV) infection, during which circulating sICs are generated (*37, 62*). As the assay also

309 enables the sensitive and quantitative measurement of FcγR ligand bioactivity it allows the
310 detection of sICs not only in clinical specimens but also pharmaceutical preparations of IgG
311 and Fc-fusion proteins for therapeutic use (*46*). The presence of ICs in therapeutic
312 preparations or sIC formation following patient treatment is unwanted due to the risk of side
313 effects such as lupus-like syndrome which has been linked to mAb treatment in patients
314 receiving infliximab (*63*) or bevacizumab (*64*), both mAbs used in this study. As this assay is
315 highly sensitive to any aggregation of IgG, it also represents a tool to control the purity,
316 quality and stability of mAb preparations produced for therapeutic use in patients. In addition,
317 the assessment of sIC-mediated FcγR activation allows for optimization of mAbs and Fc-
318 fusion proteins regarding their molecular design and manufacturing. Specifically, Fc-
319 molecules targeting cytokines and soluble factors, which result in sIC formation, could be
320 designed for reduced or enhanced FcγR activation such as glyco-engineered mAbs or LALA-
321 mutant mAbs (*65, 66*). Notably, the scalability of this cell-based test system does allow for
322 large-scale screening of samples.
323
324 *sICs form FcγR ligands with distinct functional profiles*
325 While immobilized ICs decorating infected cells, viral particles or microbial surfaces restrict
326 their triggering effect to a single immune cell residing in very close vicinity, sICs can rapidly
327 disseminate reaching a high number of immune effector cells thus developing a systemic
328 effect with far reaching and long-lasting or even threatening consequences for the host as a
329 whole. This could explain the very tight control of sIC governed effector programs and the
330 unresponsiveness of activating receptors like FcγRI and IIA. We also observed a difference in
331 the response patterns for FcγRIIIA and FcγRII/B/C depending on the solubility of clustered
332 IgG (immobilized versus soluble ICs) which we validated for FcγRIIIA using primary human
333 NK cells (Fig. 4 and 5C). Importantly,only multimeric but not dimeric sICs can trigger FcγR
334 activation. This highlights the fundamental structural influence of the particular antigen as

335 well as the IgG molecule on sIC dimension and subsequent FcγR-mediated signal processing.
336 The ability of the here described assay to define and quantify the activation of individual
337 FcγRs by sIC ligands is not achievable using primary immune cells due to redundant immune
338 responses upon FcγR activation and complex, overlapping expression pattern of FcγRs.
339 Finally, and in contrast to primary human cells, murine BW5147 reporter cells are largely
340 inert to human cytokines, which provides a key advantage to measure FcγR activation
341 selectively in human samples. Notably, the two basically sIC-responsive human FcγR types,
342 i.e. FcγRIIIA and FcγRIIB, are either highly activating versus strongly inhibitory and thus
343 show a mutually exclusive expression pattern (ref. review, z.B. Ravetch und Falk). FcγRIIIA
344 mediates ADCC elicited by NK cells and the induction of a pro-inflammatory cytokine profile
345 by $CD16^{+}$ monocytes, while FcγRIIIB is a GPI-anchored receptor on neutrophils. FcγRIIB is
346 an inhibitory receptor expressed by B cells and dendritic cells (DCs) regulating B cell
347 activation, antibody production by plasma cells and the activation state of DCs, while the
348 activating FcγRIIC is found on NK cells mediating ADCC. However, as FcγRIIC is only
349 expressed by roughly 10% of the human population, its role is still poorly understood (*49-52*).
350 Given the here shown fundamental difference in FcγR reactivity towards multimeric sICs
351 versus immobilized IgG it is tempting to speculate that FcγRIIIA- and FcγRIIB/C-positive
352 immune cells might have evolved to differentially perceive these different FcγR ligands (sICs
353 versus membrane bound insoluble ICs) and translate them into distinct reaction patterns. This
354 could be achieved by differences in receptor density, signal transduction or regulation of
355 receptor expression. Consulting the literature indeed supports our hypothesis with neutrophils,
356 B cells and NK cells being efficiently activated by sICs via almost identical receptor
357 ectodomains (*18, 28, 67, 68*), while the immunological outcome of their triggering very much
358 differs.
359
360

361

362 *Dynamic sIC size measurement and monitoring of bioactivity in sIC-associated diseases*

363 We provide for the first time a simultaneous functional and biophysical assessment of the
364 paradigmatic Heidelberger-Kendall precipitation curve (*12, 13*). While previous work already
365 revealed that large and small sICs differentially impacts IL-6 production in PBMCs (*6*), the
366 dynamics of FcγR activation resulting from constant changes in sIC size have not been
367 explored on a systematic basis. This was undertaken in this study by directly analyzing
368 synthetic ICsformed by highly pure recombinant components via AF4 (Fig. 5A, Fig. S2,
369 Table S1). Our data document that sIC size is indeed governed by antibody:antigen ratios
370 covering a wide range of sizes up to several megadaltons. In the presence of increasing
371 amounts of antibody or antigen deviating from an optimal antibody:ratio, sIC size steadily
372 decreases. Further, by the measurement of FcγR activation we now translate sIC size directly
373 to asimple but precise read-out. In doing so, we show that sIC size essentially tunes FcγR
374 activation on and off. Thus, our new test system can not only contribute to the functional
375 detection and quantification of clinically relevant sICs but also provides a starting point on
376 how to avoid pathological consequences by influencing the sIC size, for example by
377 administering therapeutic antibodies or recombinant antigens in optimized concentrations,
378 thus becoming relevant in clinical pharmacokinetics.

379

380 *Limitations of the reporter system and conclusions*

381 While it is known that FcγRIIA requires FcγRIIIB or FcRn to efficiently respond to ICs (*22,*
382 *23, 69*), unexpectedly, we found that FcγRI is not activated by sICs in our assay. We assume
383 that FcγRI interaction with sICs might require a native cellular environment given that a
384 major function of this FcγR is the uptake and processing of antigen via ICs even in the
385 absence of a signaling motif (*21*). However, we find that FcγRI ectodomains alone are not
386 responsive to sICs implying a thoroughly different cross-linking threshold for FcγRI

387 compared with FcγRIIB and IIIA. This feature is possibly linked to its molecular architecture
388 being the only high-affinity FcγR with three extracellular Ig domains compared to the two
389 domains found in other FcγRs with lower affinity to monomeric IgG. This observation also
390 reflects a general consideration regarding the BW5147 reporter system. While providing a
391 robust and uniform read-out using a scalable cell-based approach, the assay is not able to
392 reflect native immune cell functions governed by cell-intrinsic signalling cascades. The major
393 advancements of this reporter system include i) a higher accuracy regarding FcγR activation
394 compared to merely affinity measurements, ii) an sIC size dependent quantification of FcγR
395 responsiveness and iii) the identification of FcγR activating sICs in autoimmunity and
396 infection. Finally, this scalable, sensitive and robust system to detect FcγR activating sICs in
397 clinical samples might enable their identification in diseases that have not been linked to sIC-
398 mediated pathology, yet.
399
400 **Materials and Methods**
401
402 *Cell culture:* All cells were cultured in a 5% CO_2 atmosphere at 37°C. BW5147 mouse
403 thymoma cells (BW, obtained from ATCC: TIB-47) were maintained at $3x10^5$ to $9x10^5$
404 cells/ml in Roswell Park Memorial Institute medium (RPMI GlutaMAX, Gibco)
405 supplemented with 10% (vol/vol) fetal calf serum (FCS, Biochrom), sodium pyruvate (1x,
406 Gibco) and β-mercaptoethanol (0.1 mM, Gibco). 293T-CD20 (kindly provided by Irvin Chen,
407 UCLA (*70*)) were maintained in Dulbecco's modified Eagle's medium (DMEM, Gibco)
408 supplemented with 10% (vol/vol) FCS.
409
410 *FcγR receptor activation assay:* FcγR activation was measured adapting a previously
411 described cell-based assay (*45, 71*). The assay was modified to measure FcγR activation in
412 solution. Briefly, $2x10^5$ mouse BW-FcγR (BW5147) reporter cells were incubated with

413 synthetic sICs or diluted serum in a total volume of 100 µl for 16 h at 37°C and 5% CO_2.
414 Incubation was performed in a 96-well ELISA plate (Nunc maxisorp) pre-treated with
415 PBS/10% FCS (v/v) for 1 h at 4°C. Immobilized IgG was incubated in PBS on the plates prior
416 to PBS/10% FCS treatment. Reporter cell mIL-2 secretion was quantified via ELISA as
417 described (*45*).
418
419 *Recombinant antigens and monoclonal antibodies to form sICs:* Recombinant human (rh)
420 cytokines TNF, IL-5, and VEGFA were obtained from Stem Cell technologies. Recombinant
421 CD20 was obtained as a peptide (aa141-188) containing the binding region of rituximab
422 (Creative Biolabs). FcγR-specific mAbs were obtained from Stem Cell technologies (CD16:
423 clone 3G8; CD32: IV.3). Reverse sICs were generated from these receptor-specific antibodies
424 using goat-anti-mouse IgG $F(ab)_2$ fragments (Invitrogen) in a 1:1 ratio. Pharmaceutically
425 produced humanized monoclonal IgG1 antibodies infliximab (Ifx), bevacizumab (Bvz),
426 mepolizumab (Mpz) and rituximab (Rtx) were obtained from the University Hospital
427 Pharmacy Freiburg. Mouse anti-hTNFα (IgG2b, R&D Systems, 983003) was used to generate
428 sICs reactive with mouse FcγRs. sICs were generated by incubation of antigens and
429 antibodies in reporter cell medium or PBS for 2 h at 37°C.
430
431 *Lentiviral transduction:* Lentiviral transduction of BW5147 cells was performed as described
432 previously (*47, 55*). In brief, chimeric FcγR-CD3ζ constructs (*45*) were cloned into a
433 pUC2CL6IPwo plasmid backbone. For every construct, one 10-cm dish of packaging cell line
434 at roughly 70% density was transfected with the target construct and two supplementing
435 vectors providing the VSV gag/pol and VSV-G-env proteins (6 µg of DNA each) using
436 polyethylenimine (22.5 µg/ml, Sigma) and Polybrene (4 µg/ml; Merck Millipore) in a total
437 volume of 7 ml (2 ml of a 15-min-preincubated transfection mix in serum-free DMEM added
438 to 5 ml of fresh full DMEM). After a medium change, virus supernatant harvested from the

439 packaging cell line 2 days after transfection was then incubated with target BW cells
440 overnight (3.5 ml of supernatant on 10^6 target cells), followed by expansion and pool
441 selection using complete medium supplemented with 2 µg/ml of puromycin (Sigma) over a
442 one week culture period.
443
444 *BW5147 toxicity test:* Cell counting was performed using a Countess II (Life Technologies)
445 according to supplier instructions. Cell toxicity was measured as a ratio between live and dead
446 cells judged by trypan blue staining over a 16 h time frame in a 96well format (100 µl volume
447 per well). BW5147 cells were mixed 1:1 with Trypan blue (Invitrogen) and analysed using a
448 Countess II. rhTNFα was diluted in complete medium.
449
450 *human IgG suspension ELISA:* 1 µg of IgG1 (rituximab in PBS, 50 µl/well) per well was
451 incubated on a 96well microtiter plate (NUNC Maxisorp) pre-treated (2h at RT) with PBS
452 supplemented with varying percentages (v/v) of FCS (PAN Biotech). IgG1 bound to the
453 plates was detected using an HRP-conjugated mouse-anti-human IgG mAb (Jackson
454 ImmunoResearch).
455
456 *BW5147 cell flow cytometry:* BW5147 cells were harvested by centrifugation at 900 g and RT
457 from the suspension culture. $1x10^6$ cells were stained with PE- or FITC-conjugated anti-
458 human FcγR mAbs (BD) or a PE-TexasRed-conjugated human IgG-Fc fragment (Rockland)
459 for 1h at 4°C in PBS/3%FCS. After 3 washing steps in PBS/3%FCS, the cells were
460 transferred to Flow cytometry tubes (BD) and analysed using BD LSR Fortessa and FlowJo
461 (V10) software.
462
463 *NK cell activation flow cytometry:* PBMC were purified from donor blood using Lymphocyte
464 separation Media (Anprotec). Primary NK cells were separated from donor PBMCs via

465 magnetic bead negative selection (Stem Cell technologies) and NK cell purity was confirmed
466 via staining of CD3 (Biolegend, clone HIT3a), CD16 (Biolegend, clone 3G8) and CD56
467 (Miltenyi Biotec, clone AF12-7H3). 96well ELISA plates (Nunc Maxisorp) were pre-treated
468 with PBS/10% FCS (v/v) for 1 h at 4°C. NK cells were stimulated in pre-treated plates and
469 incubated at 37°C and 5% CO_2 for 4 h. Golgi Plug and Golgi Stop solutions (BD) were added
470 as suggested by supplier. CD107a (APC, BD, H4A3) specific conjugated mAb was added at
471 the beginning of the incubation period. Following the stimulation period, MIP-1β (PE, BD
472 Pharmigen), IFNγ (BV-510, Biolegends, 4SB3) and TNFα (PE/Cy7, Biolegends, MAB11)
473 production was measured via intracellular staining Cytokines (BD, CytoFix/CytoPerm, Kit as
474 suggested by the supplier). 50 ng/ml PMA (InvivoGen) + 0.5 µM Ionomycin (InvivoGen)
475 were used as a positive stimulation control for NK cell activation. After 3 washing steps in
476 PBS/3%FCS, the cells were transferred to Flow cytometry tubes (BD) and analysed using a
477 BD FACS Fortessa and FlowJo (V10) software. FcγRII or FcγRIII block was performed by
478 addition of receptor specific mAbs (Stem cell technologies, IV.3 and 3G8) at a 1:100 dilution
479 at the beginning of the incubation period. Cells were transferred to Flow cytometry tubes
480 (BD) and analyzed using BD LSR Fortessa and FlowJo (V10) software.
481
482 *Asymmetric flow field flow fractionation (AF4):* The AF4 system consisted of a flow
483 controller (Eclipse AF4, Wyatt), a MALS detector (DAWN Heleos II, Wyatt), a UV detector
484 (1260 Infinity G1314F, Agilent) and the separation channel (SC channel, PES membrane, cut-
485 off 10 kDa, 490 µm spacer, wide type, Wyatt). Elution buffer: 1.15 g/L Na_2HPO_4 (Merck),
486 0.20 g/L NaH_2PO_4 x H_2O (Merck), 8.00 g/L NaCl (Sigma) and 0,20 g/L NaN_3 (Sigma),
487 adjusted to pH 7.4, filtered through 0.1 µm. AF4 sequence (Vx = cross flow in mL/min): (a)
488 elution (2 min, Vx: 1.0); (b) focus (1 min, Vx: 1.0), focus + inject (1 min, Vx: 1.0, inject flow:
489 0.2 mL/min), repeated three times; (c) elution (30 min, linear Vx gradient: 1.0 to 0.0); (d)
490 elution (15 min, Vx: 0.0); (e) elution + inject (5 min, Vx: 0.0). A total protein mass of 17±0.3

491 μg (Ifx, rhTNFα or ICs, respectively) was injected. The eluted sample concentration was
492 calculated from the UV signal at 280 nm using extinction coefficients of 1.240 mL/(mg cm)
493 or 1.450 mL/(mg cm) in the case of TNFα or Ifx, respectively. For the ICs, extinction
494 coefficients were not available and difficult to calculate as the exact stoichiometry is not
495 known. An extinction coefficient of 1.450 mL/(mg cm) was used for calculating the molar
496 masses of all ICs. Especially in the case of ICs rich in TNFα, the true coefficients should be
497 lower, and the molar masses of these complexes are overestimated by not more than 14 %.
498 The determined molar masses for TNFα-rich complexes are therefore biased but the observed
499 variations in molar mass for the different ICs remain valid. The mass-weighted mean of the
500 distribution of molar masses for each sample was calculated using the ASTRA 7 software
501 package (Wyatt).
502
503 *SLE patient cohort:* Sera from patients with SLE were obtained from the Immunologic,
504 Rheumatologic Biobank (IR-B) of the Department of Rheumatology and Clinical
505 Immunology. Biobanking and the project were approved by the local ethical committee of the
506 University of Freiburg (votes 507/16 and 624/14). All patients who provided blood to the
507 biobank had provided written informed consent. Ethical Statement: The study was designed in
508 accordance with the guidelines of the Declaration of Helsinki (revised 2013). Patients with
509 SLE (n = 25) and healthy controls (n = 4) were examined. All patients met the revised ACR
510 classification criteria for SLE. Disease activity was assessed using the SLEDAI-2K score.
511 C3d levels were analyzed in EDTA plasma using rocket double decker immune-
512 electrophoresis with antisera against C3d (Polyclonal Rabbit Anti-Human C3d Complement,
513 Agilent) and C3c (Polyclonal Rabbit Anti-Human C3c Complement Agilent) as previously
514 described (*72*). Anti-human dsDNA antibodies titers were determined in serum using an anti-
515 dsDNA IgG ELISA kit (diagnostik-a GmbH).
516

517 *Patient serum IC precipitation:* For polyethylene glycol (PEG) precipitation human sera were
518 mixed with PEG 6000 (Sigma-Aldrich) in PBS at a final concentration of 10% PEG 6000.
519 After overnight incubation at 4°C, ICs were precipitated by centrifugation at 2000 x g for
520 30 min at 4 °C, pellets were washed once with PEG 6000 and then centrifugated at 2000 x g
521 for 20 min at 4 °C. Supernatants were harvested and precipitates re-suspended in pre-warmed
522 PBS for 1 h at 37 °C. IgG concentrations of serum, precipitates and supernatants obtained
523 after precipitation were quantified by Nanodrop (Thermo Scientific™) measurement.
524
525 *Mice and Models:* Animal experiments were approved by the local governmental commission
526 for animal protection of Freiburg (Regierungspräsidium Freiburg, approval no. G16/59 and
527 G19/21). Lupus-prone (NZBxNZW)F1 mice (NZB/WF1) were generated by crossing
528 NZB/BlNJ mice with NZW/LacJ mice, purchased from The Jackson Laboratory. KRNtg mice
529 were obtained from F. Nimmerjahn (Universität Erlangen-Nürnberg) with the permission of
530 D. Mathis and C. Benoist (Harvard Medical School, Boston, MA), C57BL/6 mice (BL/6) and
531 NOD/ShiLtJArc (NOD/Lt) mice were obtained from the Charles River Laboratories. K/BxN
532 (KRNtgxNOD)F1 mice (K/BxN) were obtained by crossing KRNtg mice and NOD/Lt mice.
533 All mice were housed in a 12-h light/dark cycle, with food and water ad libitum. Mice were
534 euthanized and blood collected for serum preparation from 16 weeks old BL/6 animals, from
535 16 weeks old arthritic K/BxN animals and from 26 – 38 weeks old NZB/WF1 mice with
536 established glomerulonephritis.
537
538 *Statistical analyses:* Statistical analyses were performed using Graphpad Prism software (v6)
539 and appropriate tests.
540
541
542

Acknowledgements: We thank T. Schleyer (IR-B Biobank) for providing patient samples. We are indebted to Falk. Nimmerjahn (Universität Erlangen-Nürnberg) for providing KRNtg mice. **Funding:** This work was supported by an intramural junior investigator fund of the Faculty of Medicine to PK (EQUIP - Funding for Medical Scientists, Faculty of Medicine, University of Freiburg), by the German Research foundation (DFG) (FOR2830 HE 2526/9-1) to HH, by the DFG research grant TRR130 to REV and the Ministry of Science, Research, and Arts Baden-Württemberg (Margarete von Wrangell Programm) to NC. **Author contributions:** HC and PK designed and developed the reporter system, conducted Fc-gamma receptor activation experiments and prepared synthetic immune complexes. AMP, US and REV manage the SLE patient cohort, provided sera and performed immune complex precipitation as well as IgG quantification. MH designed and performed AF4 analyses. NC manages the mouse models and provided sera. HH and PK supervised all experiments. HC and PK analysed and interpreted data. PK wrote the paper assisted by HC, AMP, MH, NC, REV and HH. **Competing interests:** The authors declare no financial and non-financial competing interests. **Data and materials availability:** All data associated with this study are present in the paper or Supplementary Materials.

Supplementary Materials

Fig. S1. rhTNFα is not toxic to mouse lymphocyte BW5147 cells even at high concentrations.

Fig. S2. AF4 elution profiles of Ifx/TNFα-immune complexes.

Table S1. Analysis of the molar mass distribution of ICs from AF4 data.

566 **References**

567 1. L. L. Lu, T. J. Suscovich, S. M. Fortune, G. Alter, Beyond binding: antibody effector
568 functions in infectious diseases. *Nat Rev Immunol* **18**, 46-61 (2018).
569 2. J. V. Ravetch, S. Bolland, IgG Fc receptors. *Annu Rev Immunol* **19**, 275-290 (2001).
570 3. C. E. van der Poel, R. M. Spaapen, J. G. van de Winkel, J. H. Leusen, Functional
571 characteristics of the high affinity IgG receptor, FcgammaRI. *J Immunol* **186**, 2699-
572 2704 (2011).
573 4. P. Bruhns *et al.*, Specificity and affinity of human Fcgamma receptors and their
574 polymorphic variants for human IgG subclasses. *Blood* **113**, 3716-3725 (2009).
575 5. D. Urlaub *et al.*, Activation of natural killer cells by rituximab in granulomatosis with
576 polyangiitis. *Arthritis Res Ther* **21**, 277 (2019).
577 6. A. Lux, X. Yu, C. N. Scanlan, F. Nimmerjahn, Impact of immune complex size and
578 glycosylation on IgG binding to human FcgammaRs. *J Immunol* **190**, 4315-4323
579 (2013).
580 7. F. Kiefer *et al.*, The Syk protein tyrosine kinase is essential for Fc gamma receptor
581 signaling in macrophages and neutrophils. *Mol Cell Biol* **18**, 4209-4220 (1998).
582 8. Y. Luo, J. W. Pollard, A. Casadevall, Fcgamma receptor cross-linking stimulates cell
583 proliferation of macrophages via the ERK pathway. *J Biol Chem* **285**, 4232-4242
584 (2010).
585 9. S. Greenberg, P. Chang, S. C. Silverstein, Tyrosine phosphorylation of the gamma
586 subunit of Fc gamma receptors, p72syk, and paxillin during Fc receptor-mediated
587 phagocytosis in macrophages. *J Biol Chem* **269**, 3897-3902 (1994).
588 10. S. Bournazos, T. T. Wang, R. Dahan, J. Maamary, J. V. Ravetch, Signaling by
589 Antibodies: Recent Progress. *Annu Rev Immunol* **35**, 285-311 (2017).
590 11. F. Nimmerjahn, J. V. Ravetch, Antibody-mediated modulation of immune responses.
591 *Immunol Rev* **236**, 265-275 (2010).
592 12. M. Heidelberger, F. E. Kendall, A Quantitative Study of the Precipitin Reaction
593 between Type Iii Pneumococcus Polysaccharide and Purified Homologous Antibody.
594 *J Exp Med* **50**, 809-823 (1929).
595 13. M. Heidelberger, F. E. Kendall, The Precipitin Reaction between Type Iii
596 Pneumococcus Polysaccharide and Homologous Antibody : Iii. A Quantitative Study
597 and a Theory of the Reaction Mechanism. *J Exp Med* **61**, 563-591 (1935).
598 14. A. M. Duchemin, L. K. Ernst, C. L. Anderson, Clustering of the High-Affinity Fc
599 Receptor for Immunoglobulin-G (Fc-Gamma-Ri) Results in Phosphorylation of Its
600 Associated Gamma-Chain. *J Biol Chem* **269**, 12111-12117 (1994).
601 15. A. Getahun, J. C. Cambier, Of ITIMs, ITAMs, and ITAMis: revisiting immunoglobulin
602 Fc receptor signaling. *Immunol Rev* **268**, 66-73 (2015).
603 16. P. Bruhns, F. Jonsson, Mouse and human FcR effector functions. *Immunol Rev* **268**,
604 25-51 (2015).
605 17. P. Bruhns, Properties of mouse and human IgG receptors and their contribution to
606 disease models. *Blood* **119**, 5640-5649 (2012).
607 18. F. Nimmerjahn, J. V. Ravetch, Fcgamma receptors as regulators of immune
608 responses. *Nat Rev Immunol* **8**, 34-47 (2008).
609 19. F. Nimmerjahn, J. V. Ravetch, Fcgamma receptors: old friends and new family
610 members. *Immunity* **24**, 19-28 (2006).
611 20. M. Guilliams, P. Bruhns, Y. Saeys, H. Hammad, B. N. Lambrecht, The function of
612 Fcgamma receptors in dendritic cells and macrophages. *Nat Rev Immunol* **14**, 94-108
613 (2014).
614 21. Z. K. Indik *et al.*, The high affinity Fc gamma receptor (CD64) induces phagocytosis in
615 the absence of its cytoplasmic domain: the gamma subunit of Fc gamma RIIIA
616 imparts phagocytic function to Fc gamma RI. *Exp Hematol* **22**, 599-606 (1994).
617 22. G. Fossati, R. C. Bucknall, S. W. Edwards, Insoluble and soluble immune complexes
618 activate neutrophils by distinct activation mechanisms: changes in functional
619 responses induced by priming with cytokines. *Ann Rheum Dis* **61**, 13-19 (2002).

620 23. J. J. Hubbard *et al.*, FcRn is a CD32a coreceptor that determines susceptibility to IgG
621 immune complex-driven autoimmunity. *J Exp Med* **217**, (2020).
622 24. A. Pincetic *et al.*, Type I and type II Fc receptors regulate innate and adaptive
623 immunity. *Nat Immunol* **15**, 707-716 (2014).
624 25. G. Vidarsson, G. Dekkers, T. Rispens, IgG subclasses and allotypes: from structure
625 to effector functions. *Front Immunol* **5**, 520 (2014).
626 26. M. Z. Tay, K. Wiehe, J. Pollara, Antibody-Dependent Cellular Phagocytosis in
627 Antiviral Immune Responses. *Front Immunol* **10**, 332 (2019).
628 27. E. A. Laborde *et al.*, Immune complexes inhibit differentiation, maturation, and
629 function of human monocyte-derived dendritic cells. *J Immunol* **179**, 673-681 (2007).
630 28. S. Kang *et al.*, IgG-Immune Complexes Promote B Cell Memory by Inducing BAFF. *J*
631 *Immunol* **196**, 196-206 (2016).
632 29. V. Granger, M. Peyneau, S. Chollet-Martin, L. de Chaisemartin, Neutrophil
633 Extracellular Traps in Autoimmunity and Allergy: Immune Complexes at Work. *Front*
634 *Immunol* **10**, 2824 (2019).
635 30. S. Berger, H. Ballo, H. J. Stutte, Immune complex-induced interleukin-6, interleukin-
636 10 and prostaglandin secretion by human monocytes: A network of pro- and anti-
637 inflammatory cytokines dependent on the antigen:antibody ratio. *Eur J Immunol* **26**,
638 1297-1301 (1996).
639 31. L. Koenderman, Inside-Out Control of Fc-Receptors. *Front Immunol* **10**, 544 (2019).
640 32. R. Plomp *et al.*, Subclass-specific IgG glycosylation is associated with markers of
641 inflammation and metabolic health. *Sci Rep* **7**, 12325 (2017).
642 33. T. C. Pierson *et al.*, The stoichiometry of antibody-mediated neutralization and
643 enhancement of West Nile virus infection. *Cell Host Microbe* **1**, 135-145 (2007).
644 34. K. R. Patel, J. T. Roberts, A. W. Barb, Multiple Variables at the Leukocyte Cell
645 Surface Impact Fc gamma Receptor-Dependent Mechanisms. *Front Immunol* **10**, 223
646 (2019).
647 35. S. Bohm, D. Kao, F. Nimmerjahn, Sweet and sour: the role of glycosylation for the
648 anti-inflammatory activity of immunoglobulin G. *Current topics in microbiology and*
649 *immunology* **382**, 393-417 (2014).
650 36. R. J. Stopforth *et al.*, Detection of Experimental and Clinical Immune Complexes by
651 Measuring SHIP-1 Recruitment to the Inhibitory FcgammaRIIB. *J Immunol* **200**, 1937-
652 1950 (2018).
653 37. T. T. Wang, J. V. Ravetch, Immune complexes: not just an innocent bystander in
654 chronic viral infection. *Immunity* **42**, 213-215 (2015).
655 38. D. H. Yamada *et al.*, Suppression of Fcgamma-receptor-mediated antibody effector
656 function during persistent viral infection. *Immunity* **42**, 379-390 (2015).
657 39. U. Antes, H. P. Heinz, D. Schultz, D. Brackertz, M. Loos, C1q-bearing immune
658 complexes detected by a monoclonal antibody to human C1q in rheumatoid arthritis
659 sera and synovial fluids. *Rheumatol Int* **10**, 245-250 (1991).
660 40. R. H. Zubler *et al.*, Circulating and intra-articular immune complexes in patients with
661 rheumatoid arthritis. Correlation of 125I-Clq binding activity with clinical and biological
662 features of the disease. *J Clin Invest* **57**, 1308-1319 (1976).
663 41. D. Koffler, V. Agnello, R. Thoburn, H. G. Kunkel, Systemic lupus erythematosus:
664 prototype of immune complex nephritis in man. *J Exp Med* **134**, 169-179 (1971).
665 42. T. V. Rajan, The Gell-Coombs classification of hypersensitivity reactions: a re-
666 interpretation. *Trends in immunology* **24**, 376-379 (2003).
667 43. S. Tahir *et al.*, A CD153+CD4+ T follicular cell population with cell-senescence
668 features plays a crucial role in lupus pathogenesis via osteopontin production. *J*
669 *Immunol* **194**, 5725-5735 (2015).
670 44. A. Bano *et al.*, CD28 (null) CD4 T-cell expansions in autoimmune disease suggest a
671 link with cytomegalovirus infection. *F1000Res* **8**, (2019).
672 45. E. Corrales-Aguilar *et al.*, A novel assay for detecting virus-specific antibodies
673 triggering activation of Fcgamma receptors. *Journal of immunological methods* **387**,
674 21-35 (2013).

675 46. H. A. D. Lagasse, H. Hengel, B. Golding, Z. E. Sauna, Fc-Fusion Drugs Have
676 FcgammaR/C1q Binding and Signaling Properties That May Affect Their
677 Immunogenicity. *AAPS J* **21**, 62 (2019).
678 47. S. Van den Hoecke *et al.*, Hierarchical and Redundant Roles of Activating
679 FcgammaRs in Protection against Influenza Disease by M2e-Specific IgG1 and
680 IgG2a Antibodies. *J Virol* **91**, (2017).
681 48. M. Tanaka *et al.*, Activation of Fc gamma RI on monocytes triggers differentiation into
682 immature dendritic cells that induce autoreactive T cell responses. *J Immunol* **183**,
683 2349-2355 (2009).
684 49. S. Lisi, M. Sisto, D. D. Lofrumento, S. D'Amore, M. D'Amore, Advances in the
685 understanding of the Fc gamma receptors-mediated autoantibodies uptake. *Clin Exp*
686 *Med* **11**, 1-10 (2011).
687 50. J. C. Anania, A. M. Chenoweth, B. D. Wines, P. M. Hogarth, The Human
688 FcgammaRII (CD32) Family of Leukocyte FcR in Health and Disease. *Front Immunol*
689 **10**, 464 (2019).
690 51. D. Metes *et al.*, Expression of functional CD32 molecules on human NK cells is
691 determined by an allelic polymorphism of the FcgammaRIIC gene. *Blood* **91**, 2369-
692 2380 (1998).
693 52. W. B. Breunis *et al.*, Copy number variation of the activating FCGR2C gene
694 predisposes to idiopathic thrombocytopenic purpura. *Blood* **111**, 1029-1038 (2008).
695 53. F. Vuckovic *et al.*, Association of systemic lupus erythematosus with decreased
696 immunosuppressive potential of the IgG glycome. *Arthritis Rheumatol* **67**, 2978-2989
697 (2015).
698 54. Y. Kaneko, F. Nimmerjahn, J. V. Ravetch, Anti-inflammatory activity of
699 immunoglobulin G resulting from Fc sialylation. *Science* **313**, 670-673 (2006).
700 55. P. Kolb *et al.*, Identification and Functional Characterization of a Novel Fc Gamma-
701 Binding Glycoprotein in Rhesus Cytomegalovirus. *J Virol* **93**, (2019).
702 56. U. E. Nydegger, J. S. t. Davis, Soluble immune complexes in human disease. *CRC*
703 *Crit Rev Clin Lab Sci* **12**, 123-170 (1980).
704 57. R. J. Levinsky, J. S. Cameron, J. F. Soothill, Serum immune complexes and disease
705 activity in lupus nephritis. *Lancet* **1**, 564-567 (1977).
706 58. R. J. Levinsky, Role of circulating soluble immune complexes in disease. *Arch Dis*
707 *Child* **53**, 96-99 (1978).
708 59. L. Briant, N. Coudronniere, V. Robert-Hebmann, M. Benkirane, C. Devaux, Binding of
709 HIV-1 virions or gp120-anti-gp120 immune complexes to HIV-1-infected quiescent
710 peripheral blood mononuclear cells reveals latent infection. *J Immunol* **156**, 3994-
711 4004 (1996).
712 60. S. K. Oh *et al.*, Identification of HIV-1 envelope glycoprotein in the serum of AIDS and
713 ARC patients. *J Acquir Immune Defic Syndr (1988)* **5**, 251-256 (1992).
714 61. D. A. Vuitton, L. Vuitton, E. Seilles, P. Galanaud, A plea for the pathogenic role of
715 immune complexes in severe Covid-19. *Clin Immunol* **217**, 108493 (2020).
716 62. K. Madalinski, B. Burczynska, K. H. Heermann, A. Uy, W. H. Gerlich, Analysis of viral
717 proteins in circulating immune complexes from chronic carriers of hepatitis B virus.
718 *Clin Exp Immunol* **84**, 493-500 (1991).
719 63. D. A. Wetter, M. D. Davis, Lupus-like syndrome attributable to anti-tumor necrosis
720 factor alpha therapy in 14 patients during an 8-year period at Mayo Clinic. *Mayo Clin*
721 *Proc* **84**, 979-984 (2009).
722 64. D. A. MacDonald *et al.*, Aflibercept exhibits VEGF binding stoichiometry distinct from
723 bevacizumab and does not support formation of immune-like complexes.
724 *Angiogenesis* **19**, 389-406 (2016).
725 65. K. O. Saunders, Conceptual Approaches to Modulating Antibody Effector Functions
726 and Circulation Half-Life. *Front Immunol* **10**, 1296 (2019).
727 66. T. Li *et al.*, Modulating IgG effector function by Fc glycan engineering. *Proceedings of*
728 *the National Academy of Sciences of the United States of America* **114**, 3485-3490
729 (2017).

730 67. M. R. Goodier *et al.*, Sustained Immune Complex-Mediated Reduction in CD16
731 Expression after Vaccination Regulates NK Cell Function. *Front Immunol* **7**, 384
732 (2016).
733 68. T. N. Mayadas, G. C. Tsokos, N. Tsuboi, Mechanisms of immune complex-mediated
734 neutrophil recruitment and tissue injury. *Circulation* **120**, 2012-2024 (2009).
735 69. S. Nagarajan *et al.*, Cell-specific, activation-dependent regulation of neutrophil
736 CD32A ligand-binding function. *Blood* **95**, 1069-1077 (2000).
737 70. K. Morizono *et al.*, Redirecting lentiviral vectors pseudotyped with Sindbis virus-
738 derived envelope proteins to DC-SIGN by modification of N-linked glycans of
739 envelope proteins. *J Virol* **84**, 6923-6934 (2010).
740 71. E. Corrales-Aguilar *et al.*, Human cytomegalovirus Fcgamma binding proteins gp34
741 and gp68 antagonize Fcgamma receptors I, II and III. *PLoS pathogens* **10**, e1004131
742 (2014).
743 72. E. Rother, B. Lang, R. Coldewey, K. Hartung, H. H. Peter, Complement split product
744 C3d as an indicator of disease activity in systemic lupus erythematosus. *Clin*
745 *Rheumatol* **12**, 31-35 (1993).

746

747

748 **Figures**

749

750 **Figure 1**

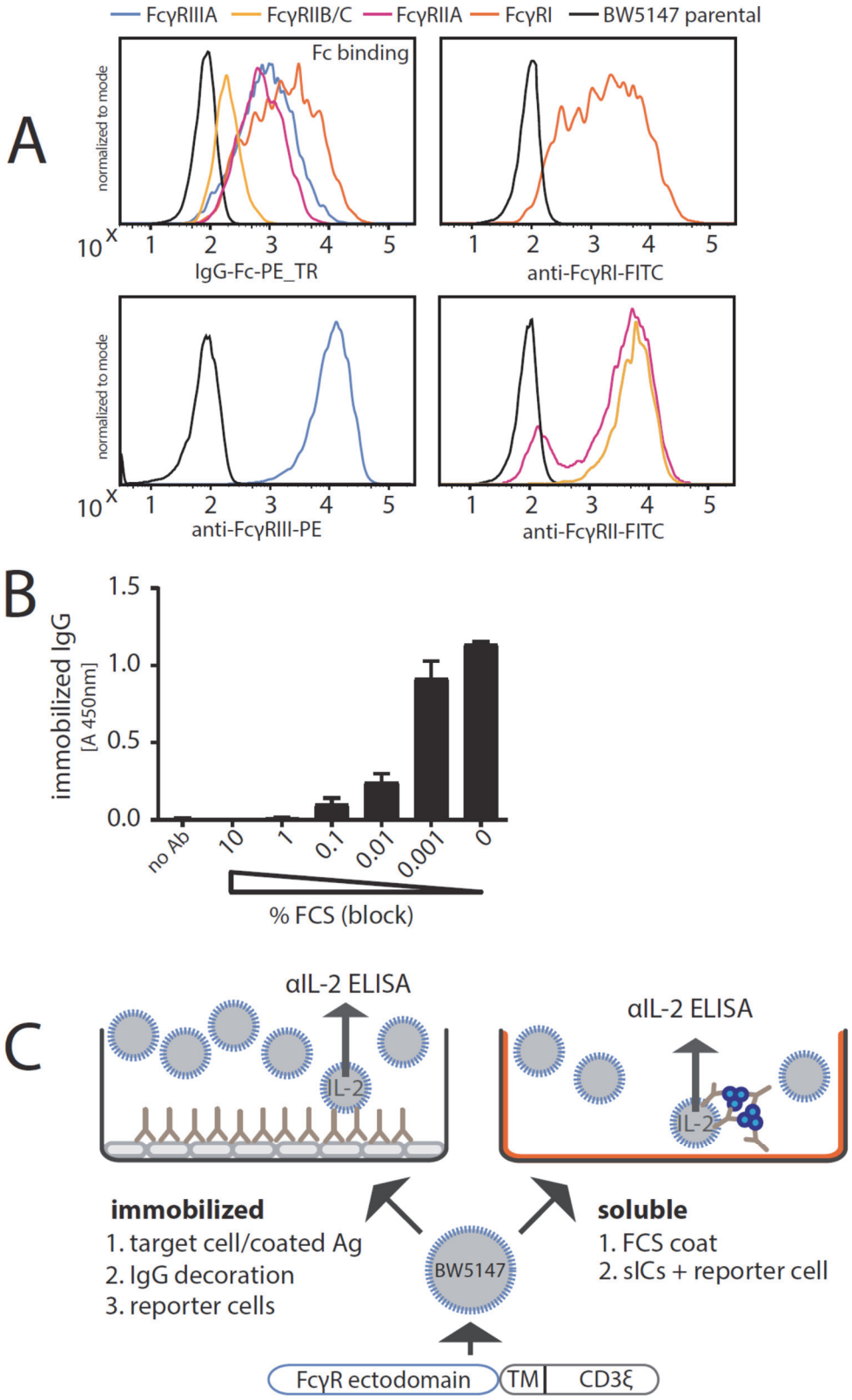

751

752

753 **Figure 2**

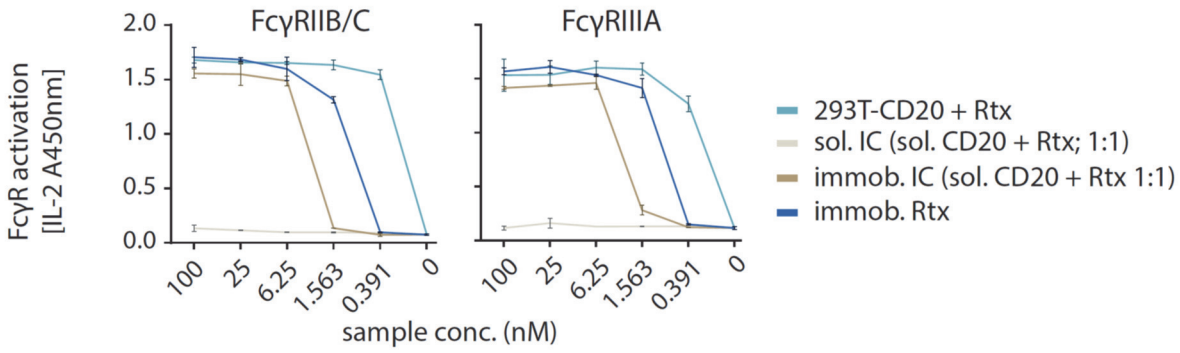

754

755 **Fig. 2. FcγRIIB/C and FcγRIIIA do not respond to small hetero-dimeric sICs but are**
756 **sensitive to immobilized IgG/ICs.** Dose-dependent activation of FcγR-bearing reporter cells
757 by immobilized IC can be mimicked by immobilized IgG. Response curves of human
758 FcγRIIB/C and FcγRIIIA are similar between opsonized cells (293T cells stably expressing
759 CD20 + Rtx), immobilized IC (rec. soluble CD20 + Rtx) and immobilized IgG (Rtx). sIC
760 formed by monovalent antigen (rec. soluble CD20) do not activate human FcγRs. X-Axis
761 shows sample concentration determined by antibody molarity. Y-Axis shows FcγR activation
762 determined by reporter cell IL-2 production.

763

764 **Figure 3**

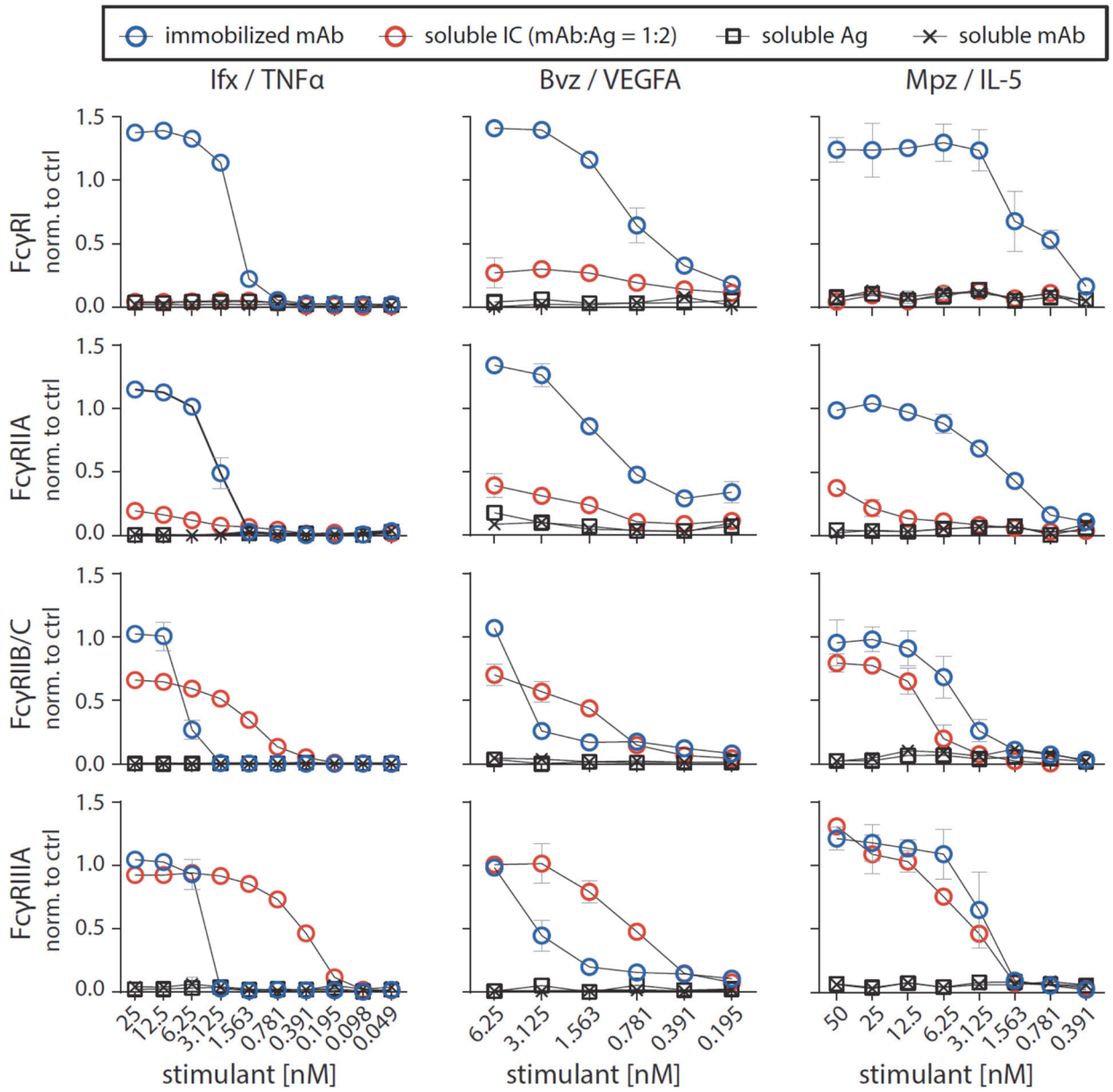

765
766

767 **Fig. 3. FcγRIIB/C and FcγRIIIA are activated by sICs formed from multivalent**
768 **antigens.** Three different multivalent ultra-pure antigens (Ag) mixed with respective therapy-
769 grade mAbs were used to generate sICs as indicated for each set of graphs (top to bottom). IC
770 pairs: infliximab (Ifx) and rhTNFα; mepolizumab (Mpz) and rhIL-5; bevacizumab (Bvz) and
771 rhVEGFA. X-Axis: concentrations of stimulant expressed as molarity of either mAb or Ag
772 monomer and IC (expressed as mAb molarity) at a mAb:Ag ratio of 1:2. Soluble antigen or
773 soluble antibody alone served as negative controls and were not sufficient to activate human
774 FcγRs. FcγR responses were normalized to immobilized rituximab (Rtx) at 1µg/well (set to 1)
775 and a medium control (set to 0). All FcγRs show dose-dependent activation towards
776 immobilized IgG. FcγRIIA shows low activation at high sIC concentrations compared to
777 immobilized IgG activation. FcγRI shows no activation towards sICs. FcγRIIIA and
778 FcγRIIB/C are dose-dependently activated by sICs with responses comparable in strength to
779 immobilized IgG stimulant. Experiments performed in technical replicates. Error bars = SD.
780 Error bars smaller than symbols are not shown.

781 **Figure 4**

782

783

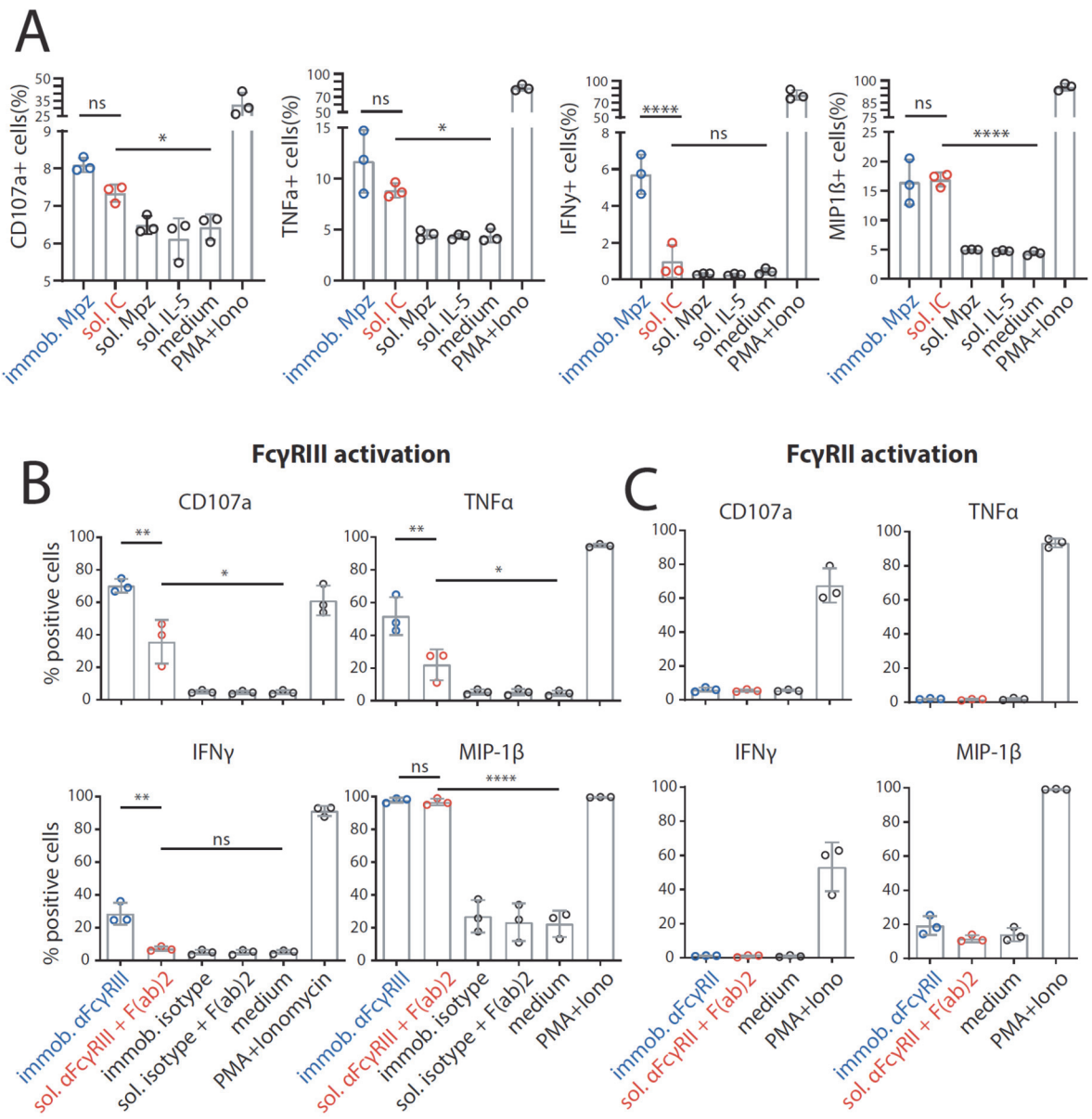

784

785

786

787 **Fig. 4. The FcγRIII-dependent activation pattern of primary NK cells depends on IC**
788 **solubility**. Negatively selected primary NK cells purified from PBMCs of three healthy
789 donors were tested for NK cell activation markers. Error bars = SD. Two-way ANOVA
790 (Turkey). A) NK cells were incubated with immobilized IgG (mepolizumab, Mpz), soluble IC
791 (Mpz:IL-5 = 1:1), soluble Mpz or soluble IL-5 (all at 200 nM, 10^6 cells). Incubation with
792 PMA and Ionomycin (Iono) served as a positive control. Incubation with medium alone
793 served as a negative control. B) NK cells were incubated for 4 h with immobilized FcγRIII-
794 specific mAb, soluble mouse-anti-human IgG $F(ab)_2$ complexed FcγRIII-specific mAb
795 (reverse sICs), immobilized IgG of non-FcγRIII-specificity (isotype control) or soluble $F(ab)_2$
796 complexed isotype control (all at 1µg, 10^6 cells). Incubation with PMA and Ionomycin served
797 as a positive control. Incubation with medium alone served as a negative control. C) As in B
798 using an FcγRII-specific mAb. NK cells from the tested donors in this study do not react to
799 FcγRII activation.

800 **Figure 5**

801

802

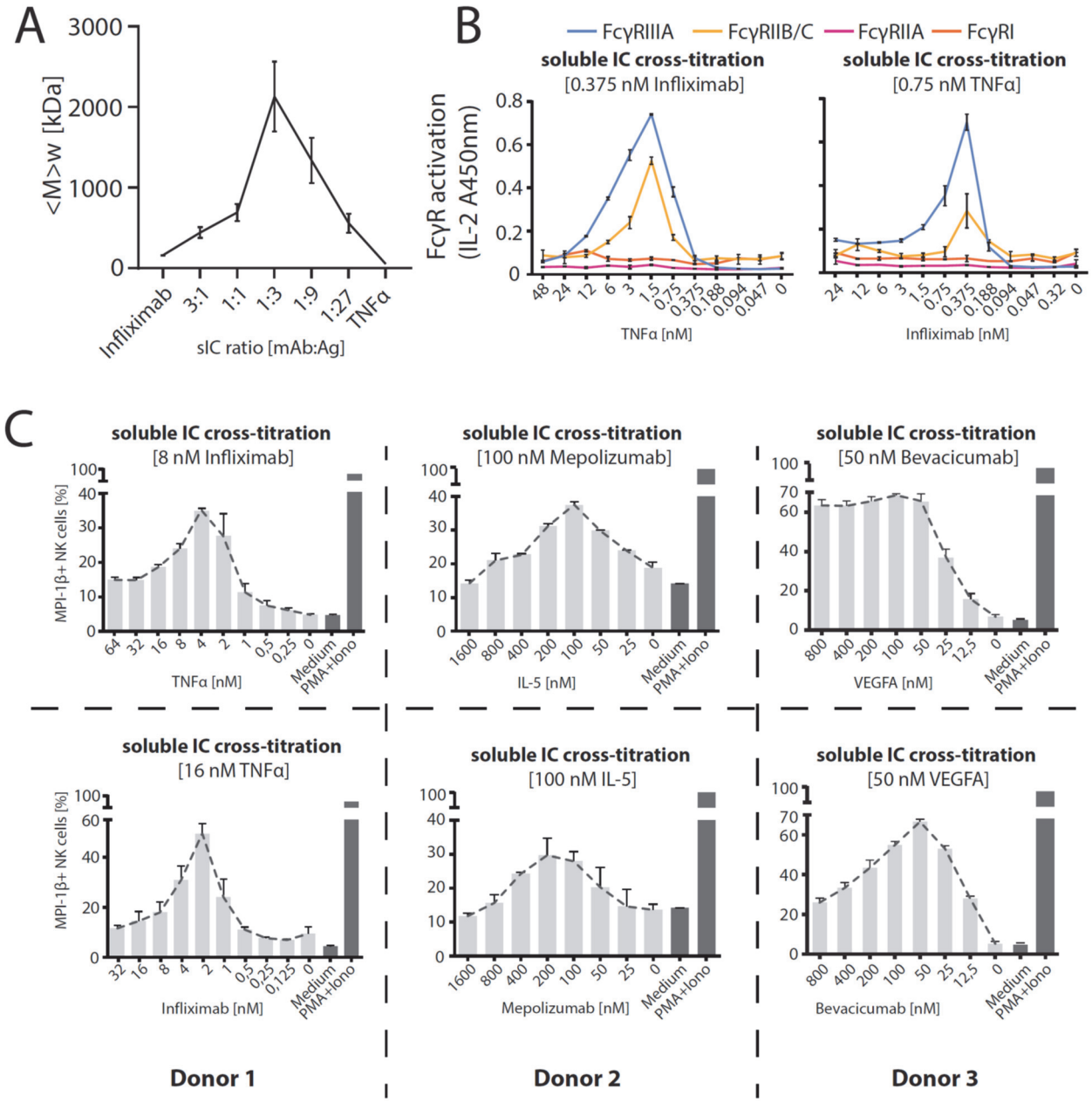

803

804

805 **Fig. 5. FcγRIIB/C and FcγR-IIIA respond to sIC size reproducing a Heidelberger-**
806 **Kendall like precipitation curve.** A) infliximab (mAb) and rhTNFα (Ag) were mixed at
807 different ratios (17 µg total protein, calculated from monomer molarity) and analysed via
808 AF4. sIC size is maximal at a 1:3 ratio of mAb:Ag and reduced when either mAb or Ag are
809 given in excess. $\langle M \rangle_w$ = mass-weighted mean of the molar mass distribution. Three
810 independent experiments. Error bars = SD. Data taken from Table S1. One complete run
811 analysis is shown in Fig. S2. B) FcγR BW5147 reporter cell activation is sensitive to sIC size.
812 sICs of different size were generated by cross-titration according to the AF4 determination.
813 Reporter cells were incubated with fixed amounts of either mAb (infliximab, left) or Ag
814 (rhTNFα, right) and titrated amounts of antigen or antibody, respectively. X-Axis shows
815 titration of either antigen or antibody, respectively (TNFα calculated as monomer). IL-2
816 production of reporter cells shows a peak for FcγRIIB/C and FcγRIIIA activation at an
817 antibody:antigen ratio between 1:2 and 1:4. FcγRs I and IIA show no activation towards sICs
818 in line with previous observations, see Fig.3. Two independent experiments. Error bars = SD.
819 C) Purified primary NK cells from three different donors were incubated with cross-titrated
820 sICs as in A. NK cells were measured for MIP-1β expression (% positivity). Incubation with
821 PMA and Ionomycin served as a positive control. Incubation with medium alone served as a
822 negative control. Measured in technical replicates. Error bars = SD.

823 **Figure 6**

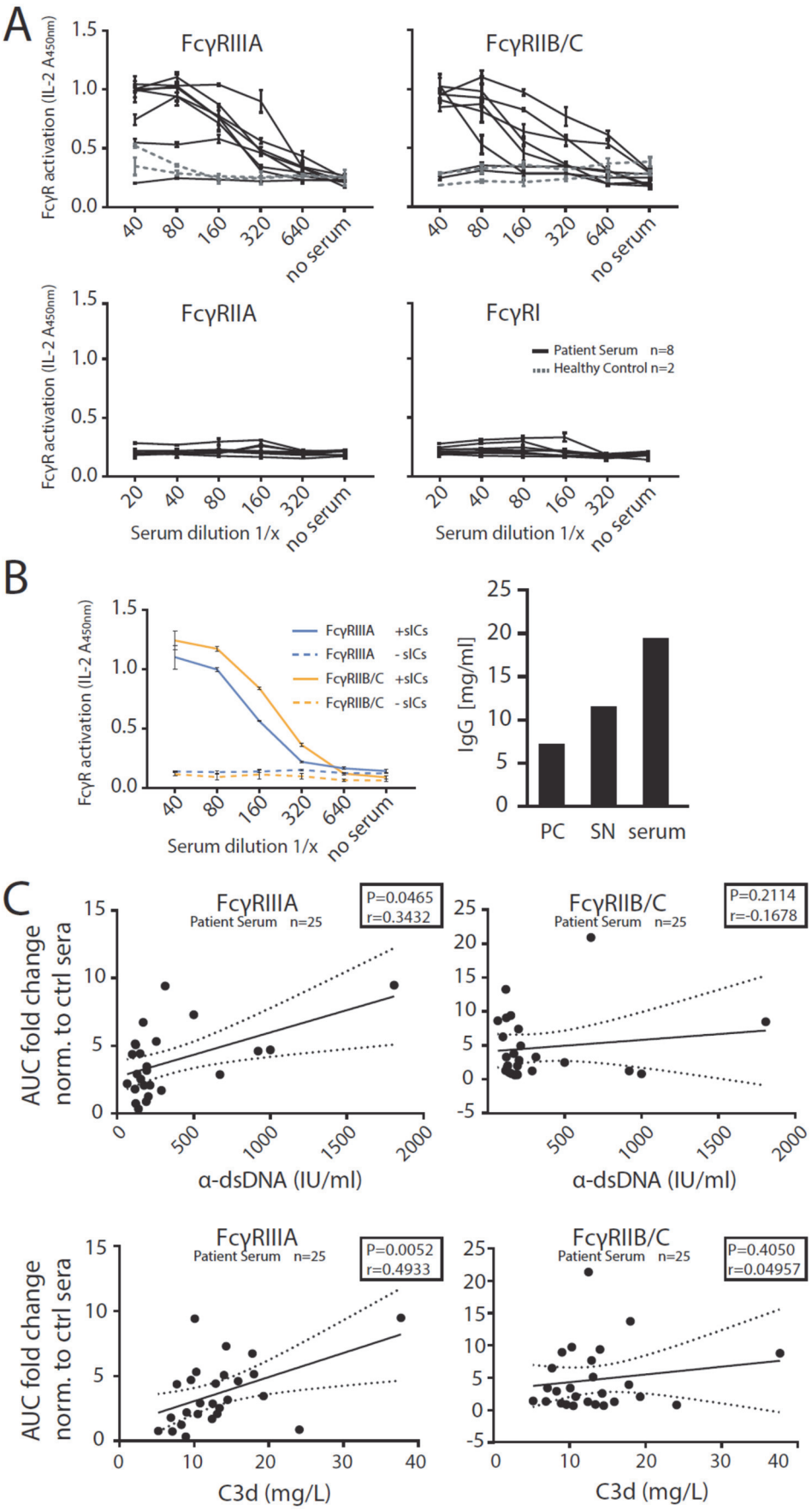

824

825 **Fig. 6. The reporter assay enables quantification of serum-derived sICs from SLE**
826 **patients.** Serum derived sIC from systemic lupus erythematosus (SLE) patients activate
827 human FcγR reporter cells. 25 patients and 4 healthy control individuals were separated into
828 three groups for measurement. A) Experiments shown for an exemplary group of 8 SLE
829 patients and two healthy individuals. Dose-dependent reactivity of FcγRs IIIA and IIB/C was
830 observed only for SLE patient sera and not for sera from healthy individuals. FcγRs I and IIA
831 show no reactivity towards clinical IC in line with previous observations. B) Activation of
832 FcγRs IIB/C and IIIA by patient serum is mediated by serum derived sICs. Patient serum
833 samples were depleted of sICs by PEG precipitation and the supernatant (SN) was compared
834 to untreated serum regarding FcγR activation (left). Performed in technical replicates. IgG
835 concentration in the precipitate (PC), supernatant (SN) or unfractionated serum respectively is
836 shown in the bar graph (right). IC precipitation did leave non-complexed IgG in the
837 supernatant. C) FcγRIIIA activation, but not FcγRIIB/C activation, significantly correlates
838 with known SLE disease markers. FcγR activation data from A was correlated to established
839 SLE disease markers (α-dsDNA levels indicated as IU/ml or C3d concentrations indicated as
840 mg/L). FcγR activation from a dose-response curve as in A was calculated as area under curve
841 (AUC) for each SLE patient (n=25) or healthy individual (n=4) and expressed as fold change
842 compared to the healthy control mean. SLE patients with α-dsDNA levels below 50 IU/ml
843 and C3d values below 6 mg/L were excluded. One-tailed Spearman's.
844
845

846 **Figure 7**

847

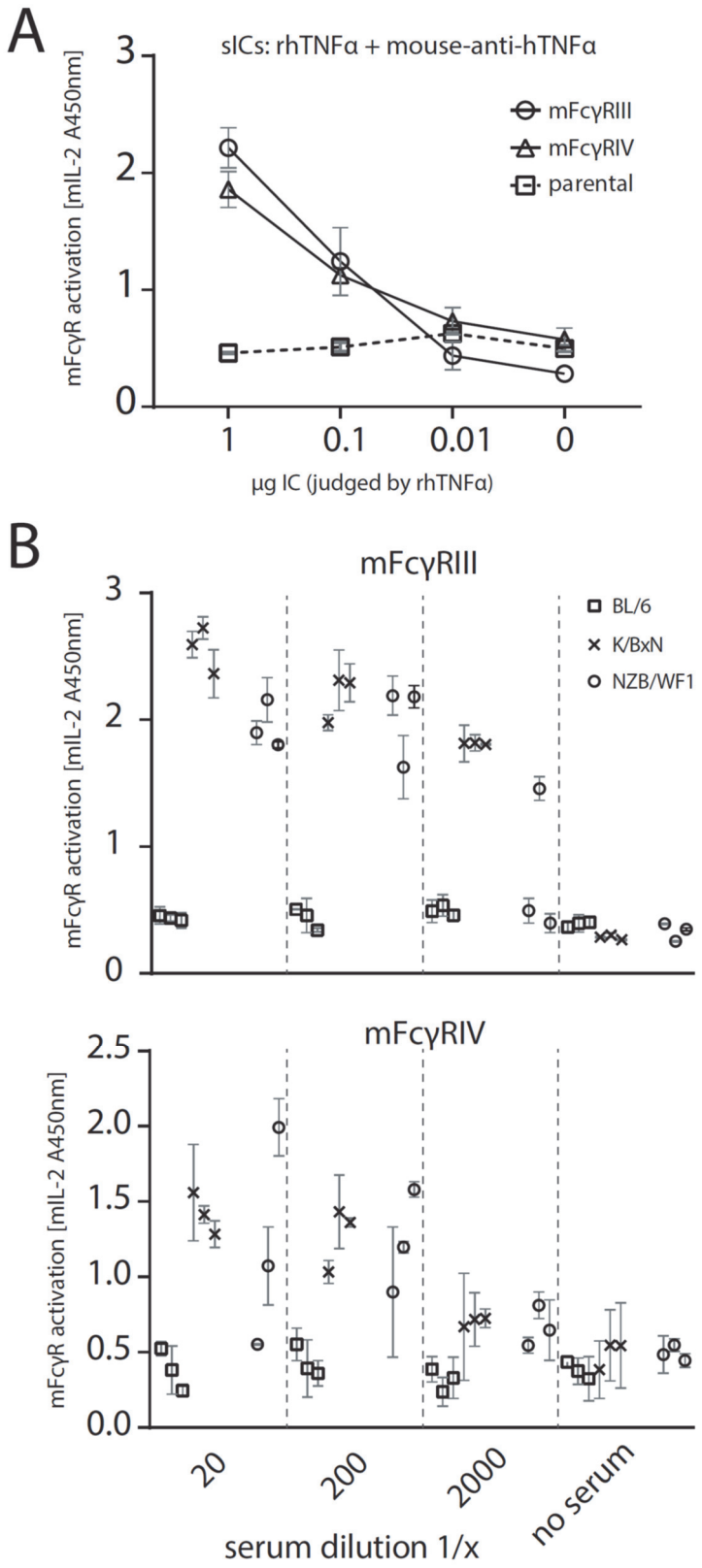

848

849

850 **Fig. 7. The reporter assay can be applied to mouse models of autoimmune disease.** A)
851 Reporter cells expressing mFcγRIII, mFcγRIV or parental BW5147 cells were incubated with
852 titrated amounts of synthetic sICs generated from rhTNFα and mouse-anti-hTNFα at a 1:1
853 ratio by mass. One experiment in technical replicates. Error bars = SD. B) Titrations of 3
854 mouse sera per group (C57BL/6, K/BxN or NZB/WF1) were incubated with mFcγR reporter
855 cells and FcγR activation was assessed as described above. Sera from BL/6 mice served as
856 negative control. Performed in technical replicates. Error bars = SD.
857
858

-Supplementary Material-

Figure S1

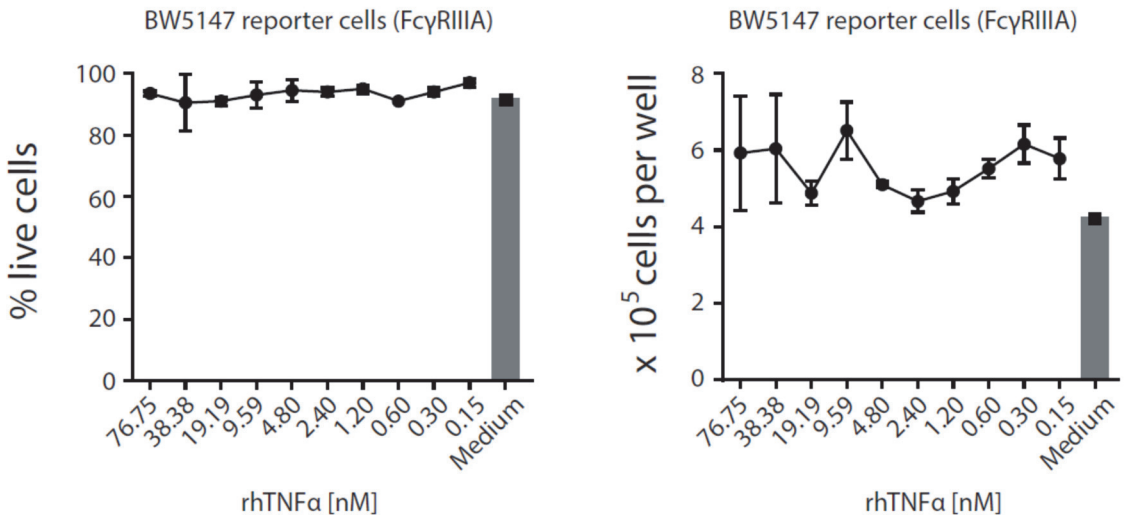

Fig. S1. rhTNFα is not toxic to mouse lymphocyte BW5147 cells even at high concentrations. Cell count and percentage of live cells were unaltered over a 16 h time frame of reporter cell culture in the presence of indicated rhTNFα concentrations and comparable to regular growth in complete medium. Experiments were conducted in 3 replicates. Error bars = SD.

871 **Figure S2**

872

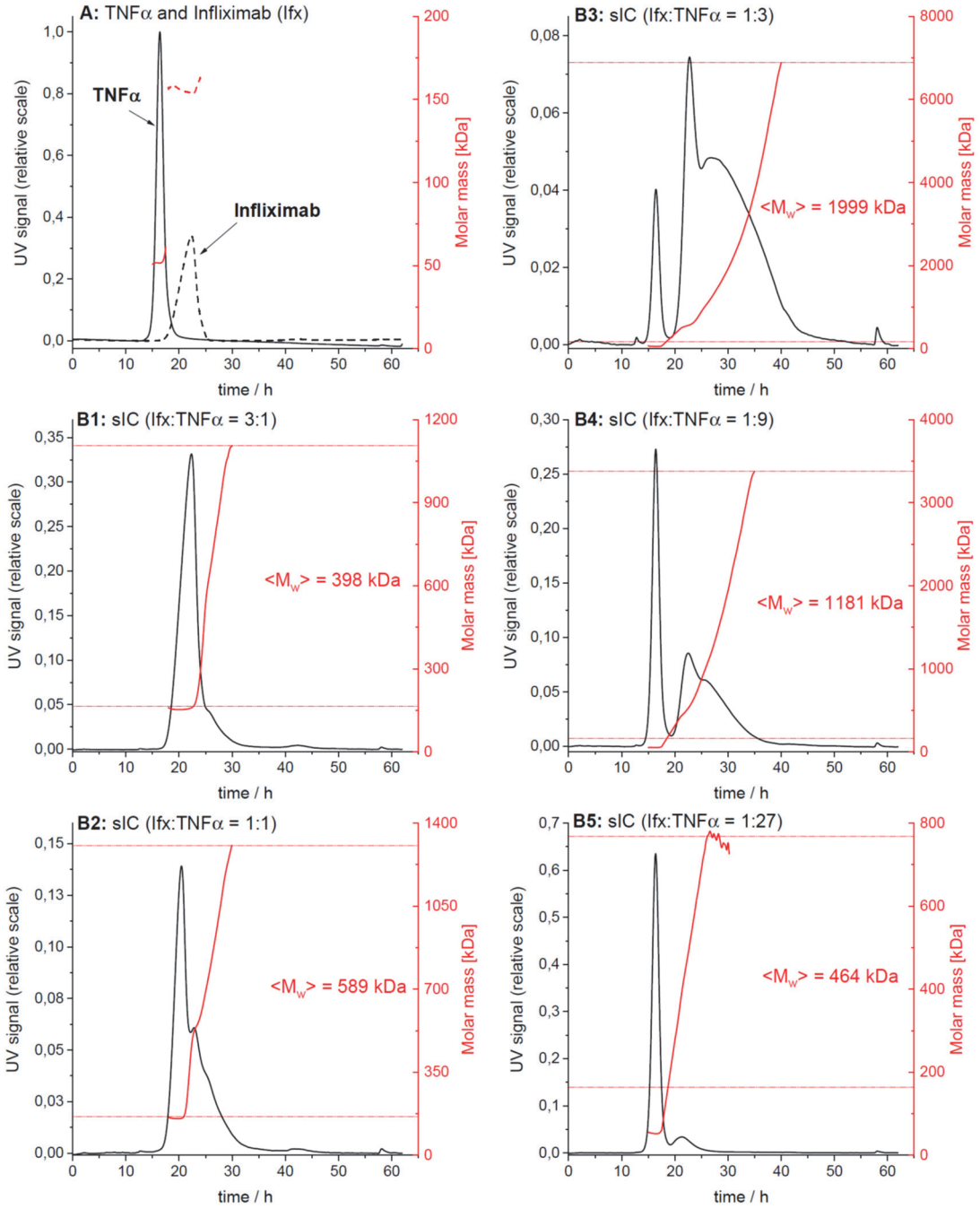

873

874

875 **Fig. S2. AF4 elution profiles of Ifx/TNFα-immune complexes.**

876 The elution profiles from one of three independent runs are shown. Protein concentration in
877 the eluate is shown in black (UV signal at λ = 280 nm, normalized to the highest UV signal
878 found in this experiment), molar masses determined by MALS for a given retention time in
879 red. Horizontal red lines indicate the range of molar masses used to calculate the mass-
880 weighted mean of molar masses $<M_w>$. A) Overlay of the elution profiles obtained for TNFα
881 and Ifx, respectively; B1 to B5) Elution profiles for sICs formed after incubation of TNFα and
882 Ifx at different molar ratios.

883

884 **Table S1**

Sample	Range of assigned molar masses [kDa]			Mass-weighted mean of assigned molar masses [kDa]			
	Run 1	Run 2	Run 3	Run 1	Run 2	Run 3	Mean ± SD
Infliximab, IFX	158 – 182	153 – 164	159 – 193	162	156	163	160 ± 4
TNF -alpha	52 – 55	51 – 61	52 – 62	52	52	52	52 ± 0
Immune complexes							
IFX/TNF 3:1	182 – $1.16 \cdot 10^3$	164 – $1.11 \cdot 10^3$	193 – $1.10 \cdot 10^3$	409	398	518	442 ± 66
IFX/TNF 1:1	182 – $2.06 \cdot 10^3$	164 – $1.31 \cdot 10^3$	193 – $1.42 \cdot 10^3$	801	589	681	690 ± 106
IFX/TNF 1:3	182 – $5.05 \cdot 10^3$	164 – $6.89 \cdot 10^3$	193 – $10.8 \cdot 10^3$	$1.77 \cdot 10^3$	$2.00 \cdot 10^3$	$2.61 \cdot 10^3$	$2.13 \cdot 10^3$ ± 435
IFX/TNF 1:9	182 – $5.36 \cdot 10^3$	164 – $3.38 \cdot 10^3$	193 – $3.51 \cdot 10^3$	$1.66 \cdot 10^3$	$1.18 \cdot 10^3$	$1.17 \cdot 10^3$	$1.34 \cdot 10^3$ ± 279
IFX/TNF 1:27	182 – $1.68 \cdot 10^3$	164 – 768	193 – $1.01 \cdot 10^3$	689	464	521	558 ± 117

885

886 **Table S1. Analysis of the molar mass distribution of ICs from AF4 data.**

887 For a given elution time, the AF4 profiles provide the concentration (UV) at which a given
888 molar mass (MALS) of a protein is present in the sample. The molar mass distribution of Ifx,
889 TNFα and their immune complexes (sICs) was obtained by plotting the cumulative frequency
890 as a function of molar mass. For a selected range of molar masses, a mass-weighted mean
891 value ($<M_w>$) was calculated. All detected molar masses were selected in the case of Ifx and
892 TNFα whereas only molar masses larger than the maximal molar mass found for Ifx were
893 assigned to sICs. The table shows the range of assigned molar masses and the calculated
894 $<M_w>$ for each AF4 run (n = 3).